Recombination dynamics in ultraviolet light-emitting diodes with Si-doped Al$_x$Ga$_{1-x}$N/Al$_y$Ga$_{1-y}$N multiple quantum well active regions

K. X. Chen and Y. A. Xi
Future Chips Constellation, Department of Physics, Applied Physics, and Astronomy,
Rensselaer Polytechnic Institute, Troy, New York 12180

F. W. Mont and J. K. Kim
Future Chips Constellation, Department of Electrical, Computer, and Systems Engineering,
Rensselaer Polytechnic Institute, Troy, New York 12180

E. F. Schubert[a)]
Future Chips Constellation, Department of Physics, Applied Physics, and Astronomy,
Department of Electrical, Computer, and Systems Engineering, Rensselaer Polytechnic Institute,
Troy, New York 12180

W. Liu, X. Li, and J. A. Smart
Crystal IS, Inc., 70 Cohoes Avenue, Green Island, New York 12183

Ultraviolet (UV) light-emitting diodes with Al$_x$Ga$_{1-x}$N/Al$_y$Ga$_{1-y}$N multiple quantum well active regions, doped in the barriers with different Si doping levels, show a sharp near-band edge emission line (UV luminescence). Some samples have a broad subband gap emission band centered at about 500 nm (green luminescence) in addition to the near-band edge emission. The electroluminescence intensities of the UV and green emission line are studied as a function of the injection current. For the sample grown on the AlN substrate under optimized growth conditions, the UV luminescence intensity increases linearly with the injection current, following a power law with an exponent of 1.0, while the green luminescence intensity increases sublinearly with the injection current. On the contrary, the samples grown on the sapphire substrate show a superlinear (to the power of 2.0) and linear (to the power of 1.0) dependence on the injection current for the UV and green luminescence, respectively. A theoretical model is proposed to explain the relationship between the luminescence intensities and the injection current. The results obtained from the model are in excellent agreement with the experimental results. The model provides a method to evaluate the dominant recombination process by measuring the exponent of the power-law dependence. © 2007 American Institute of Physics. [DOI: 10.1063/1.2736312]

I. INTRODUCTION

Ultraviolet (UV) light-emitting devices (LEDS) with emission wavelengths shorter than 360 nm have attracted much attention because of their applications in biochemical agent detection, high-density data storage, water purification, UV curing, and white light generation.[1–4] For these applications, sharp and strong near-band edge UV emission is desired. However, besides the near-band edge emission, parasitic subband gap emissions are often observed in UV LEDs, especially a broad visible emission band centered at around 500 nm. Otsuka *et al.* proposed that the 500 nm band in UV LEDs emitting at 339 nm is due to nitrogen vacancies.[2] Adivarahan *et al.* reported that the 250 nm near-band edge emission of AlGaN UV LEDs was accompanied by a broad visible emission band centered at about 500 nm, which was attributed to deep level transitions.[3] Park *et al.* concluded that the broad visible emission near 500 nm was derived from defect-related luminescence emitted from the AlGaN well and barrier layers of the multiple quantum wells (MQWs).[4]

In this article, we present the electroluminescence (EL) study of UV LEDs with Si-doped Al$_x$Ga$_{1-x}$N/Al$_y$Ga$_{1-y}$N MQW active regions. A detailed study is performed on the EL intensities of the UV and subband gap green emission as a function of injection current. A theoretical model is proposed to explain the relationship between the luminescence intensities and the injection current. The model is based on three different types of recombination processes and it reveals distinct power-law dependences versus injection current when monomolecular or bimolecular recombination dominates.

II. EXPERIMENTS

The UV LEDs are grown by using an Aixtron 200/4 RF-S metalorganic vapor-phase epitaxy system. Trimethylgallium, trimethylaluminum, and ammonia are used as precursors for Ga, Al, and N, respectively. Bis-cyclopentadienylmagnesium and silane (SiH$_4$) are used for *p*-type and *n*-type doping, respectively. The LED structure is shown in the inset of Fig. 1. Two sets of AlGaN/AlN superlattices are employed as a buffer layer to eliminate cracking, improve the crystalline quality, and improve electrical properties of *n*-type Al$_{0.3}$Ga$_{0.7}$N grown on top of it.[5] The MQW
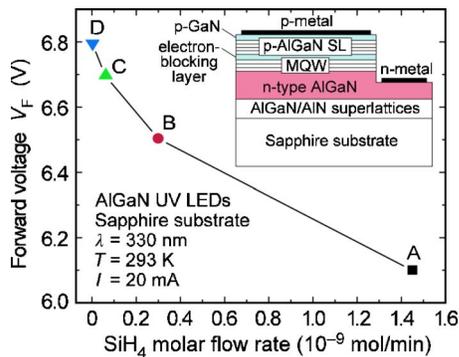
a)Electronic mail: efschubert@rpi.edu

FIG. 1. (Color online) Forward voltage at 20 mA dc injection current for UV LEDs with different Si doping levels in the MQW barriers (sample A: high doping; sample B: medium doping; sample C: low doping; sample D: no doping). The inset shows the UV LED structure.

structure consists of four periods of $Al_{0.1}Ga_{0.9}N$ (3 nm, well)/ $Al_{0.17}Ga_{0.83}N$ (7 nm, barrier). The barriers are doped with Si whereas the wells are left undoped. Four MQW UV LED samples emitting at 330 nm are grown on the (0001) plane of sapphire substrates, with the barriers of the MQW doped using four different SiH_4 flow rates. The SiH_4 molar flow rates for the four samples are: 1.45×10^{-9} mol/min (sample A, high doping); 2.9×10^{-10} mol/min (sample B, medium doping); 5.94×10^{-11} mol/min (sample C, low doping); and 0 mol/min (sample D, no doping). On top of the MQW, there is a 20 nm p-type $Al_{0.4}Ga_{0.6}N$ electron-blocking layer. Finally, a 10 period Mg-doped $Al_{0.13}Ga_{0.87}N$ (5 nm)/ $Al_{0.4}Ga_{0.6}N$ (2.5 nm) superlattice and a 50 nm thick Mg-doped GaN layer are grown for high p-type conductivity.[6] Besides these four samples, one more sample (sample E) emitting at 315 nm is also grown using a similar epilayer structure on a bulk AlN substrate under optimized growth conditions. Ni (20 nm)/Au (35 nm) and Ti (20 nm)/Al (100 nm)/Ti (45 nm)/Au (55 nm) are deposited by using electron-beam deposition to serve as p-type and n-type Ohmic contacts, respectively. Standard photolithography, deposition, and etching procedures are employed for the fabrication of the UV LEDs.

After the fabrication, the UV LEDs are wafer tested using a Karl Suss PM5 Probe Station. The direct current (dc) currents are injected by an Agilent 4155C semiconductor parameter analyzer, while the pulsed currents are injected by a Hewlett Packard 214B pulse generator. An Ocean Optics HR2000 high-resolution spectrometer is used to measure the luminescence spectrum, with an optical fiber collecting the emission from the backside of the chip. For the pulsed injection, a Tektronix TDS 3054B digital oscilloscope and an inductive current-to-voltage converter are used to monitor the wave function of the pulse.

III. RESULTS AND DISCUSSION

The forward voltages at 20 mA dc injection current are measured for the four samples (samples A−D) with different Si doping levels in the MQW barriers. Figure 1 shows that the forward voltage decreases with increasing Si barrier doping level, similar to the results reported by Tsai *et al.* for GaInN/GaN MQW LEDs.[7]
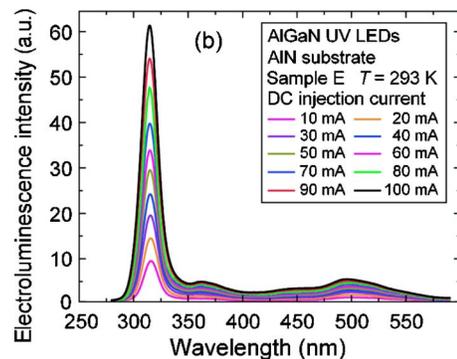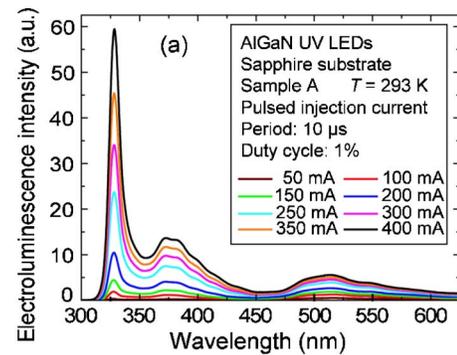

FIG. 2. (Color online) (a) EL spectrum of 330 nm UV LED (sample A) under different pulsed injection currents. The spectra of samples B, C, and D are similar with that of sample A. (b) EL spectrum of 315 nm UV LED (sample E) under different dc injection currents.

The EL spectra of the 330 nm UV LED (sample A) under different pulsed injection currents are shown in Fig. 2(a). The emission spectra of samples B, C, and D are similar with that of sample A. The period of the pulsed excitation is 10 μs and the duty cycle is 1%. Three peaks are observed in the EL spectrum: a sharp near-band edge peak at 330 nm (UV luminescence), a shoulder at 370 nm, and a broad peak centered at about 500 nm (green luminescence). The 330 nm near-band edge emission is dominant at high injection currents. The shoulder at 370 nm has been attributed to electron overshoot and recombination in p-type AlGaN layers.[8] A better carrier confinement provided by the optimized p-type AlGaN electron-blocking layer reduces the 370 nm shoulder. The broad green luminescence peak may come from defect-related deep-level transitions.[3,4] Figure 2(b) shows the electroluminescence spectrum of the 315 nm UV LED (sample E) driven under different dc injection currents. A strong near-band edge emission is observed and the green luminescence is weaker compared to the spectrum of sample A shown in Fig. 2(a). Typical emission power of the devices grown on AlN substrate is larger than 50 μW at 100 mA.

The peak intensities of the UV and green luminescence for samples A−D are depicted as a function of injection current in Figs. 3(a) and 3(b), respectively. For the UV luminescence, the peak intensities increase superlinearly with the injection current, following the power law with an exponent of 2.0. In contrast, the green luminescence peak intensity increases linearly with the injection current, with an exponent of about 1.0. This behavior is different from what is observed for the 315 nm UV LED (sample E), in which the UV luminescence peak intensity increases linearly (with an
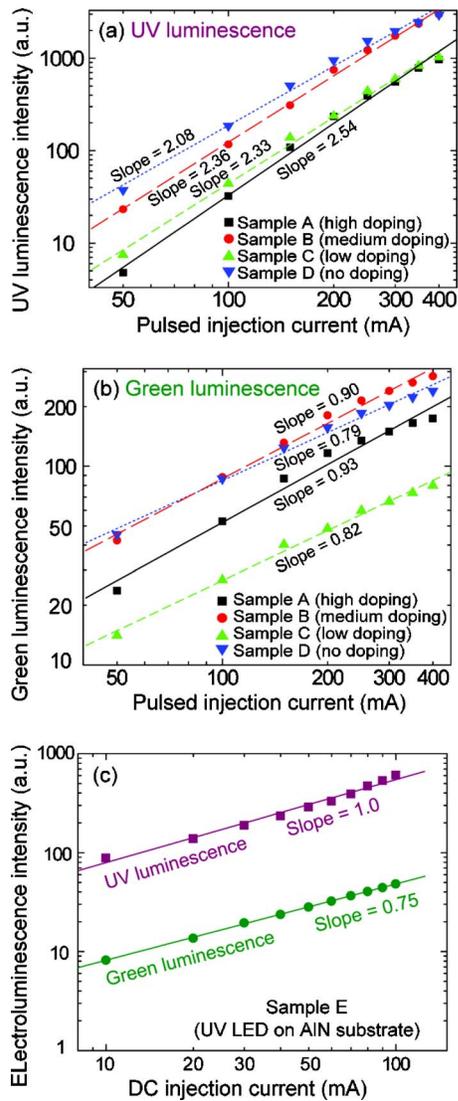
FIG. 3. (Color online) Peak intensities of (a) UV luminescence and (b) green luminescence as a function of injection current for the 330 nm UV LEDs (samples A−D). (c) Peak intensities of the UV and green luminescence as a function of injection current for the 315 nm UV LED (sample E).
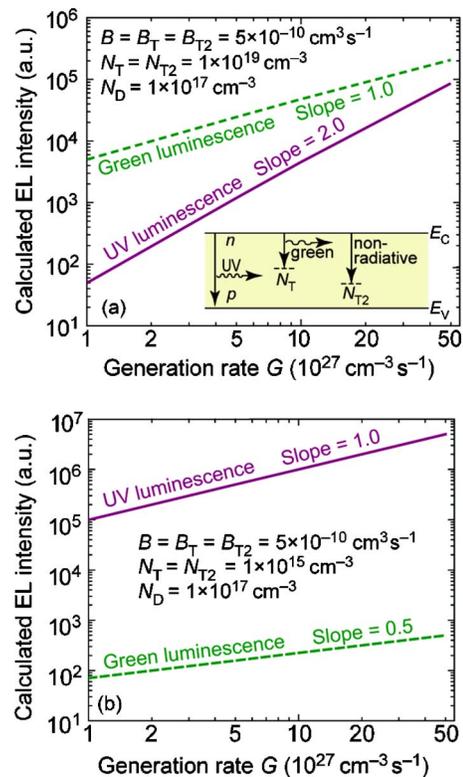

FIG. 4. (Color online) Numerically simulated dependence of UV and green luminescence intensity vs injection current when (a) monomolecular recombination dominates and (b) bimolecular recombination dominates. The inset shows three different types of recombination processes.

exponent of about 1.0) with the injection current, while the green luminescence peak intensity increases sublinearly, as shown in Fig. 3(c). For samples A−D, the slopes of both UV luminescence and green luminescence slightly increase with increasing doping levels in the barrier of the MQW. This may be due to the decreasing radiative lifetime with increasing Si doping level in the MQW.[9]

IV. THEORETICAL MODEL

Power-law dependences of the luminescence intensity measured by photoluminescence in GaN have been reported,[10–12] in which both the experimental results and the numerical simulations show that the UV luminescence increases linearly (to the power of 1.0) with the excitation power density under high-excitation conditions, while the defect-related yellow luminescence shows a square-root dependence (to the power of 1/2). Park *et al.* also observed a similar linear dependence for the UV luminescence in the EL spectrum of AlGaN UV LEDs under high injection current.[13]

Furthermore, Koleske *et al.* found that by reducing the threading dislocation density, the light output versus current dependence of the 380 nm UV LED changes from superlinear to linear.[14]

Next, a theoretical model is proposed which allows us to understand the power-law dependence of our UV LEDs. As shown in the inset of Fig. 4(a), the model considers three different recombination mechanisms: (a) a bimolecular radiative recombination between electrons (with a concentration n) and holes (with a concentration p), which emits UV light; (b) a monomolecular radiative recombination between electrons n and deep traps, N_T, which emits green light (N_T is the concentration of unoccupied radiative deep traps) and (c) a monomolecular nonradiative recombination between electrons n and deep traps, N_{T2} (N_{T2} is the concentration of unoccupied nonradiative deep traps).

The generation-recombination balance is given by[15]

$$\frac{dn}{dt} = G - \left(Bnp + B_TnN_T + B_{T2}nN_{T2}\right) = 0. \quad (1)$$

The UV and green light intensities are expressed as

$$I_{UV} = Bnp,$$

$$I_{green} = B_TnN_T. \quad (2)$$

Under high-excitation conditions, in which

$$n \approx p > N_D. \quad (3)$$

Equation (1) can be rewritten as

$$Bn^2 + (B_T N_T + B_{T2} N_{T2})n - G = 0. \tag{4}$$

By solving this equation for n, one obtains

$$n = p = \frac{-(B_T N_T + B_{T2} N_{T2}) + \sqrt{(B_T N_T + B_{T2} N_{T2})^2 + 4BG}}{2B}. \tag{5}$$

If monomolecular recombination dominates, which means

$$B_T n N_T + B_{T2} n N_{T2} \gg Bnp, \tag{6}$$

then the generation rate is approximately equal to the monomolecular recombination rate

$$G \approx B_T n N_T + B_{T2} n N_{T2}. \tag{7}$$

Therefore, $n \approx p \propto G$ and finally $I_{UV} = Bnp \propto G^2 \propto I^2$ and $I_{green} = B_T n N_T \propto G \propto I$. Here I is the injection current of the UV LED, which is related to the generation rate G by

$$G = \frac{I}{V_{active} e}, \tag{8}$$

where $e = 1.6 \times 10^{-19}$ C and V_{active} is the active region volume. The area of the UV LED is 100 μm $\times$ 100 μm and the thickness of each quantum well is 3 nm. Thus the volume of the active region is 1.2×10^{-10} cm^3.

Figure 4(a) shows the numerically simulated dependence of the UV and green luminescence intensity versus injection currents when monomolecular recombination dominates. In this figure, typical values of $B = B_T = B_{T2} = 5 \times 10^{-10}$ cm^{3}s^{-1} and $N_T = N_{T2} = 1 \times 10^{19}$ cm^{-3} are used.[12,15] The Si doping concentration is assumed to be 1×10^{17} cm^{-3}. Thus both Eqs. (3) and (6) are satisfied. Because the value of the injection current is known, the equivalent generation rate can be calculated by using Eq. (8). The simulated results show a superlinear dependence (to the power of 2.0) between the UV luminescence intensity and the injection current and a linear dependence (to the power of 1.0) between the green luminescence intensity and the injection current. These simulated results are in excellent agreement with our experimental results.

The model can also be used to explain the power-law dependence of the luminescence intensity of sample E, in which the UV luminescence increases linearly with the injection current, while the green luminescence shows a sublinear dependence. Similar behavior is also reported by other groups in the literature.[10–13] In this situation, bimolecular recombination dominates, which means

$$B_T n N_T + B_{T2} n N_{T2} \ll Bnp. \tag{9}$$

Then the generation rate is approximately equal to the bimolecular recombination rate

$$G \approx Bnp. \tag{10}$$

Therefore, $n \approx p \propto G^{1/2}$ and finally $I_{UV} = Bnp \propto G$ and $I_{green} = B_T n N_T \propto G^{1/2}$. Typical values of $B = B_T = B_{T2} = 5 \times 10^{-10}$ cm^{3}s^{-1}, $N_T = N_{T2} = 1 \times 10^{15}$ cm^{-3}, and $N_D = 1 \times 10^{17}$ cm^{-3} are used for the numerical simulation,[15] which satisfy both Eqs. (3) and (9). The numerical simulated result

is shown in Fig. 4(b). The result shows a linear dependence (to the power of 1.0) for UV luminescence intensity on generation rate G and a square-root dependence (to the power of 1/2) for the green luminescence. The results obtained from our model are consistent with our experimental results. In our calculation, Eq. (8) is being used to convert the injection current I to the equivalent generation rate G. Since the equivalent generation rate G can also be calculated in the photoluminescence if the excitation power density is known, our model can be used not only for electroluminescence but also for photoluminescence. The photoluminescence studies of GaN by Grieshaber *et al.*,[10] Xu *et al.*,[11] and Reshchikov *et al.*[12] reported a linear power law dependence on excitation density for the UV emission and a square-root dependence for the defect-related luminescence. Our model is consistent with these results when considering the equivalent generation rate G.

The earlier discussion elucidates that under different conditions, in which either monomolecular recombination or bimolecular recombination dominates, the power-law dependences of the luminescence intensity are clearly different. For the near-band edge emission, the luminescence intensity shows a superlinear dependence if monomolecular recombination dominates and a linear dependence if bimolecular recombination dominates. While for the defect-related deep-level transition, the luminescence intensity shows linear and sublinear dependence under these two conditions, respectively. Therefore, one can determine the dominant recombination process by measuring the exponent of the power-law dependence. For the 330 nm UV LED samples grown on the sapphire substrates (samples A−D), monomolecular recombination is the dominant recombination process. For the 315 nm UV LED grown on the bulk AlN substrate under optimized conditions (sample E), bimolecular recombination is the dominant recombination process. We attribute the dominance of the bimolecular recombination to a reduced density of threading dislocations in sample E, which in turn is due to the homoepitaxial growth on bulk AlN substrate. Heteroepitaxial growth of nitride layers on sapphire substrates typically results in a dislocation density varying from 10^8 to 10^{10} cm^{-2}, while homoepitaxial growth on bulk AlN substrate allows one to reduce the dislocation density by more than four orders of magnitude to $10^4 - 10^5$ cm^{-2}.[16] By reducing the threading dislocation density, the number of nonradiative recombination centers in the LEDs is reduced. Thus the dominant recombination process changes from monomolecular recombination to bimolecular recombination. Therefore, the dependence of the UV luminescence on injection current changes from a superlinear to a linear relation.[17]

V. CONCLUSION

In summary, the electroluminescence intensities of the UV and green emission line of AlGaN UV LEDs are studied as a function of the injection current. For the sample grown on the AlN substrate under optimized conditions, the UV luminescence peak intensity increases linearly with the injection current, while the green luminescence peak intensity in-

creases sublinearly. On the contrary, the samples grown on the sapphire substrate show a superlinear and linear dependence on the injection currents for the UV and green luminescence, respectively. A theoretical model is proposed to explain the relationship between the peak intensities and the injection current. The results obtained from the model are in excellent agreement with the experimental results. The model provides a method to evaluate the dominant recombination process by measuring the exponent of the power-law dependence.

[1] J. P. Zhang, S. Wu, S. Rai, V. Mandavilli, V. Adivarahan, A. Chitnis, M. Shatalov, and M. A. Khan, Appl. Phys. Lett. **83**, 3456 (2003).

[2] N. Otsuka, A. Tsujimura, Y. Hasegawa, G. Sugahara, M. Kume, and Y. Ban, Jpn. J. Appl. Phys. **39**, L445 (2000).

[3] V. Adivarahan, W. H. Sun, A. Chitnis, M. Shatalov, S. Wu, H. P. Maruska, and M. S. Khan, Appl. Phys. Lett. **85**, 2175 (2004).

[4] J. S. Park, D. W. Fothergill, P. Wellenius, S. M. Bishop, J. F. Muth, and R. F. Davis, Jpn. J. Appl. Phys., Part 1 **45**, 4083 (2006).

[5] Y. A. Xi, K. X. Chen, F. Mont, J. K. Kim, E. F. Schubert, W. Liu, X. Li, and J. A. Smart, J. Cryst. Growth **299**, 59 (2007).

[6] J. K. Kim, E. L. Waldron, Y.-L. Li, Th. Gessmann, E. F. Schubert, H. W. Jang, and J.-L. Lee, Appl. Phys. Lett. **84**, 3310 (2004).

[7] T. L. Tsai, C. S. Chang, T. P. Chen, and K. H. Huang, Phys. Status Solidi C **0**, 263 (2003).

[8] A. Chitnis, J. P. Zhang, V. Adivarahan, M. Shatalov, S. Wu, R. Pachipulusu, V. Mandavilli, and M. A. Khan, Appl. Phys. Lett. **82**, 2565 (2003).

[9] H. Haratizadeh *et al.*, Appl. Phys. Lett. **80**, 1373 (2002).

[10] W. Grieshaber, E. F. Schubert, I. D. Goepfert, R. F. Karlicek, Jr., M. J. Schurman, and C. Tran, J. Appl. Phys. **80**, 4615 (1996).

[11] H. Z. Xu, A. Bell, Z. G. Wang, Y. Okada, M. Kawabe, I. Harrison, and C. T. Foxon, J. Cryst. Growth **222**, 96 (2001).

[12] M. A. Reshchikov and R. Y. Korotkov, Phys. Rev. B **64**, 115205 (2001).

[13] J. S. Park, D. W. Fothergill, X. Zhang, Z. J. Reitmeier, J. F. Muth, and R. F. Davis, Jpn. J. Appl. Phys., Part 1 **44**, 7254 (2005).

[14] D. D. Koleske *et al.*, Appl. Phys. Lett. **81**, 1940 (2002).

[15] E. F. Schubert, *Light-Emitting Diodes*, 2nd ed. (Cambridge University Press, Cambridge, 2006).

[16] X. Hu *et al.*, Appl. Phys. Lett. **82**, 1299 (2003).

[17] K. X. Chen *et al.*, Mater. Res. Soc. Symp. Proc. **955** (2007).